



# Photodissociation spectroscopy and dynamics of Si<sub>4</sub>

Alexandra A. Hoops, Ryan T. Bise<sup>1</sup>, Hyeon Choi<sup>2</sup>, Daniel M. Neumark<sup>\*</sup>

*Department of Chemistry, University of California, Berkeley, CA 94720, USA  
Chemical Sciences Division, Lawrence Berkeley National Laboratories, Berkeley, CA 94720, USA*

Received 30 May 2001; in final form 20 July 2001

## Abstract

The photodissociation of Si<sub>4</sub> has been investigated using fast beam photofragment translational spectroscopy. The photofragment yield (PFY) spectrum shows features between 21 370 and 22 220 cm<sup>-1</sup> corresponding to the <sup>1</sup>B<sub>1u</sub> ← <sup>1</sup>X̃<sup>1</sup>A<sub>g</sub> transition that are attributed to multi-photon dissociation. Single-photon dissociation was examined at higher excitation energies ranging from 5.17 to 6.42 eV. The dominant product channel was found to be Si<sub>3</sub> + Si. Experimental photofragment translational energy distributions were modeled by phase space theory (PST), indicating statistical photodissociation with no exit barrier along the dissociation coordinate. PST modeling yields a dissociation energy of 4.60 ± 0.15 eV and Δ*H*<sub>*f,0*</sub><sup>0</sup>(Si<sub>4</sub>) = 6.75 ± 0.24 eV. © 2001 Published by Elsevier Science B.V.

## 1. Introduction

The properties of small silicon clusters have received a great deal of attention over the past two decades, with the goal of understanding how their spectroscopic and structural properties evolve with size and how large they must be to begin manifesting the electronic properties associated with bulk silicon. While there have been numerous experimental and theoretical studies of the spectroscopy and thermodynamics of Si clusters [1], there has been far less work on the photodissociation of Si clusters. The fragment mass distributions resulting from photodissociation [2–4] and

collision-induced dissociation [5] of charged Si clusters have been studied, and photodissociation cross-sections for the neutral Si<sub>*n*</sub> clusters (*n* = 18–41) have been measured [6], but there have been no photodissociation dynamics studies in which energy disposal in the products has been determined. We have developed an experiment in which reactive neutral species are generated by photodetachment of mass-selected negative ions and subsequently photodissociated, enabling measurement of photofragment yield spectrum as a function of excitation energy, the mass channels resulting from photodissociation, and the photofragment kinetic energy and angular distributions [7]. Here, this method is applied to the photochemistry and photodissociation dynamics of a neutral silicon cluster, Si<sub>4</sub>, as a means of characterizing its excited electronic states and bond dissociation energies.

The spectroscopy of the ground and excited states of Si<sub>4</sub> has been investigated by electronic absorption [8,9], Raman [10], and infrared spec-

<sup>\*</sup> Corresponding author. Fax: +1-510-642-3635.

*E-mail address:* dan@radon.cchem.berkeley.edu (D.M. Neumark).

<sup>1</sup> Current address: Bell Laboratories, Lucent Technologies, 600-700 Mountain Ave., Murray Hill, NJ 07974, USA.

<sup>2</sup> Current address: Department of Chemistry and Biochemistry, University of California, Los Angeles, CA 90095, USA.

troscopy [11] of matrix isolated  $\text{Si}_4$ . In the gas phase,  $\text{Si}_4$  has been examined spectroscopically using emission spectroscopy [12], anion photoelectron spectroscopy [13,14], and zero electron kinetic energy (ZEKE) spectroscopy [15]. These experimental studies are generally consistent with the structural and spectroscopic results from several theoretical studies [11,16–18]. Specifically,  $\text{Si}_4$  has a planar rhombus  $\tilde{X}^1A_g$  ground state with  $D_{2h}$  symmetry, and both the anion and several low-lying excited states of the neutral also have this symmetry. The combination of experiment and theory has led to a fairly complete picture of the low-lying electronic states of  $\text{Si}_4$  as shown in Fig. 1.

The experimental spectroscopic work has been complemented by thermodynamic studies on  $\text{Si}_4$  and other small Si clusters. Schmude et al. [19] measured the mass spectrum of Si clusters pro-

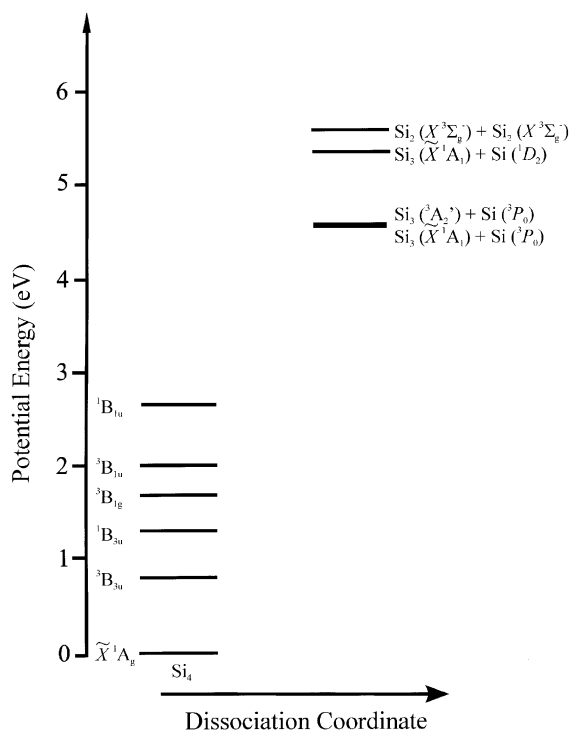


Fig. 1. Energy level diagram for  $\text{Si}_4$  and dissociation product states. The relative energetic positions of the excited singlet and triplet states are from the studies by Fulara et al. [9] and Xu et al. [14], respectively. Product state energies are based on the dissociation energy determined in this work.

duced in a high temperature Knudsen cell and determined heats of formation  $\Delta H_{f,0}^0$  for  $\text{Si}_2$ ,  $\text{Si}_3$ , and  $\text{Si}_4$ . From the latter two values,  $6.73 \pm 0.17$  and  $6.78 \pm 0.23$  eV, respectively, and the literature value of the heat of formation of Si [20], the dissociation energy  $D_0$  of  $\text{Si}_4 \rightarrow \text{Si}_3 + \text{Si}$  is calculated to be  $4.57 \pm 0.30$  eV. This value is in reasonable agreement with two theoretical studies, one using density functional theory and the other employing the Gaussian-2 (G2) procedure to calculate energetics, both yielding a fragmentation energy of 4.54 eV [21,22]. Note that a series of earlier electronic structure calculations yielded significantly higher bond dissociation energies for  $\text{Si}_4$  ranging from 5.07 to 5.472 eV [23–25].

Fig. 1 shows that all known electronic states of  $\text{Si}_4$  lie well below the lowest energy  $\text{Si}_3 + \text{Si}$  dissociation channel. The purpose of the current work on the photodissociation of mass-selected  $\text{Si}_4$  was to try to map out higher lying electronic states above the dissociation threshold, and to provide further insight into the spectroscopy, thermochemistry, and dissociation dynamics of this species. Photodissociation from excitation of the  ${}^1B_{1u} \leftarrow \tilde{X}^1A_g$  band was observed, presumably occurring via a multiphoton process since the excited state lies well below the expected dissociation threshold. Single photon dissociation was seen at higher excitation energies, and photofragment translational energy  $P(E_T)$  distributions were obtained that enabled the evaluation of product branching ratios. The measured  $P(E_T)$  distributions were then compared to those expected from phase space theory in order to determine the dissociation energy and to learn about the dissociation dynamics of  $\text{Si}_4$ .

## 2. Experiment

The experiments were performed on the fast beam photofragment translational spectrometer shown in Fig. 2. As the instrument has been described in detail previously [7,26,27], only a brief description will follow. Rotationally and vibrationally cooled  $\text{Si}_4^-$  is produced by supersonically expanding a dilute mixture of  $\text{SiH}_4$  (5%  $\text{SiH}_4$ , 95% He) through a pulsed piezoelectric valve/electrical

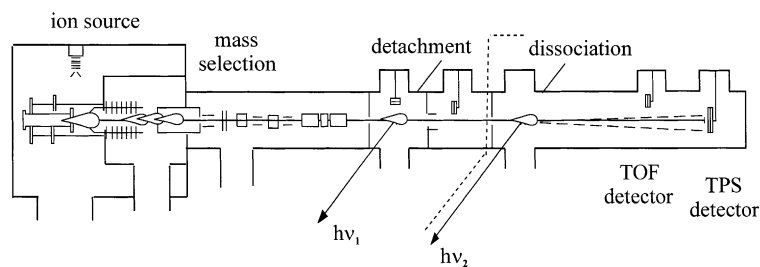


Fig. 2. Fast beam photofragment translational spectrometer.

discharge source [28]. A 1 keV electron beam downstream of the valve opening intersects the free jet expansion. The anions produced in this manner are typically accelerated to a laboratory beam energy of 6 keV, although energies as high as 8 keV can be used, and are mass-selected by time-of-flight (TOF) mass spectrometry.

$\text{Si}_4^-$  is selectively photodetached by an excimer-pumped dye laser, and undetached ions are deflected out of the beam path. Based on the adiabatic electron affinity of  $\text{Si}_4$  as determined by photoelectron spectroscopy of  $\text{Si}_4^-$  [14], a photodetachment energy of 2.46 eV was used to produce  $\text{Si}_4$  exclusively in the  $\tilde{X}^1\text{A}_g$  state. At this energy, most of the clusters will be in their ground vibrational state, with at most about one third having some excitation in the  $\nu_2$  breathing mode [14].

Following detachment, the neutral clusters are intersected by either the output of a second excimer-pumped dye laser with a bandwidth of  $0.3\text{ cm}^{-1}$ , or the output of an ArF excimer laser (193 nm). The resulting photofragments from a single parent molecule are then detected directly by either the TOF or the time and position sensing (TPS) microchannel plate (MCP) detector assembly based on the type developed by de Bruijn and Los [29]. Our implementation of this detection scheme has been described in detail elsewhere [7,26].

Two types of experiments can be performed to characterize the photodissociation of  $\text{Si}_4$ . First, the dissociation laser energy is scanned and the total flux of photofragments arriving at the TOF detector is measured, thereby producing a photofragment yield (PFY) spectrum. In the current investigation, the dissociation of  $\text{Si}_4$  from  $21\,050$  to  $22\,990\text{ cm}^{-1}$ ,  $40\,000$  to  $42\,550\text{ cm}^{-1}$ , and  $43\,860$

to  $45\,045\text{ cm}^{-1}$  was scanned. Second, the dissociation laser is tuned to specific photon energies, and dynamical information is obtained through the use of the TPS detector that employs a coincidence detection scheme. From the timing and position information obtained with the TPS detector, the masses of the fragments, their relative translational energy ( $E_T$ ), and the polar angle  $\theta$  between the relative velocity vector and the electric vector of the polarized dissociation laser are determined. The photofragment mass resolution is  $m/\Delta m \approx 10$ , while the translational energy resolution is  $\Delta E_T/E_T = 2.2\%$ . Factors that reduce the acceptance of high and low translational energy fragments are accounted for by normalizing the raw translational energy distributions with a detector acceptance function (DAF) [7].

### 3. Results and discussion

The PFY spectrum for the  $^1\text{B}_{1u} \leftarrow \tilde{X}^1\text{A}_g$  band of  $\text{Si}_4$  from  $21\,370$  to  $22\,220\text{ cm}^{-1}$  is shown in Fig. 3. Although this band lies several eV below the expected value of the dissociation energy  $\text{Si}_4$ ,  $D_0(\text{Si}_4)$ , dissociation was observed over the entirety of this region. While resolution of vibrational features was possible, no rotational structure was seen. Two vibrational progressions are observed in the spectrum with characteristic spacings of  $430$  and  $310\text{ cm}^{-1}$ .

The observed features were assigned by comparison to the matrix isolation absorption spectrum of  $\text{Si}_4$  by Fulara et al. [9]. The positions and assignments of observed peaks in the PFY spectrum are listed in Table 1. Agreement of peak

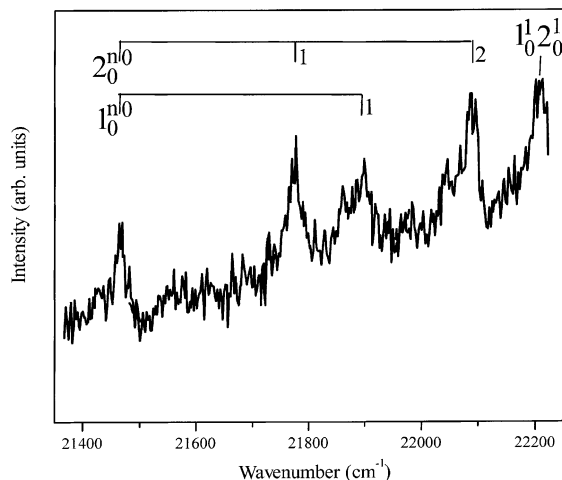


Fig. 3. Photofragment yield spectrum of the  ${}^1\text{B}_{1\text{u}} \leftarrow \tilde{\text{X}}^1\text{A}_{\text{g}}$  band of  $\text{Si}_4$ .

positions and frequencies between the two spectra indicates that the observed progressions in the PFY spectrum are due to the totally symmetric  $\nu_1$  and  $\nu_2$  modes and the combination band  $1_0^1 2_0^1$ . The PFY spectrum is shifted  $\sim 32 \text{ cm}^{-1}$  to the blue of the matrix absorption study, and the upper state vibrational frequencies agree within our experimental resolution. In contrast to the absorption spectrum, the PFY spectrum does not reach zero intensity between the vibrational features, and unstructured dissociation is observed at wavelengths greater than the origin of the  ${}^1\text{B}_{1\text{u}} \leftarrow \tilde{\text{X}}^1\text{A}_{\text{g}}$  band. The vibrationally resolved structure appears to be superimposed over a broader continuum.

Since the threshold to dissociation is projected to be approximately 2 eV above the origin of the

Table 1

Transition energies and assignments for observed peaks in the  ${}^1\text{B}_{1\text{u}} \leftarrow \tilde{\text{X}}^1\text{A}_{\text{g}}$  PFY spectrum

Transition energy ( $\text{cm}^{-1}$ )		Assignment
This work	Matrix absorption <sup>a</sup>	
21 465	21 432	$0_0^0$
21 774	21 749	$2_0^1$
21 896	21 863	$1_0^1$
22 089	22 056	$2_0^2$
22 208	22 173	$1_0^1 2_0^1$

<sup>a</sup> From Fulara et al. [9].

${}^1\text{B}_{1\text{u}} \leftarrow \tilde{\text{X}}^1\text{A}_{\text{g}}$  band, observation of dissociation from this band suggests the PFY spectrum in this region results from multi-photon absorption prior to dissociation. We also measured a non-linear dependence of PFY signal intensity upon laser fluence at  $22\,211 \text{ cm}^{-1}$  ( $1_0^1 2_0^1$  transition), consistent with multi-photon absorption. Finally, it should be noted that the observation of vibrational structure superimposed on a continuum was also seen in multi-photon dissociation of  $\text{C}_5$  [30], and that unstructured multiphoton dissociation below the dissociation threshold was seen by Mandich [6] for larger Si clusters.

Photodissociation of  $\text{Si}_4$  above 4.57 eV, the value of  $D_0(\text{Si}_4)$  determined by Schmude et al. [19] was also investigated. Efforts to observe higher electronic transitions yielded unstructured dissociation spectra over the regions of  $40\,000$  to  $42\,550 \text{ cm}^{-1}$  and  $43\,860$  to  $45\,045 \text{ cm}^{-1}$ . While PFY spectra in the intermediate region between  $42\,550 \text{ cm}^{-1}$  and

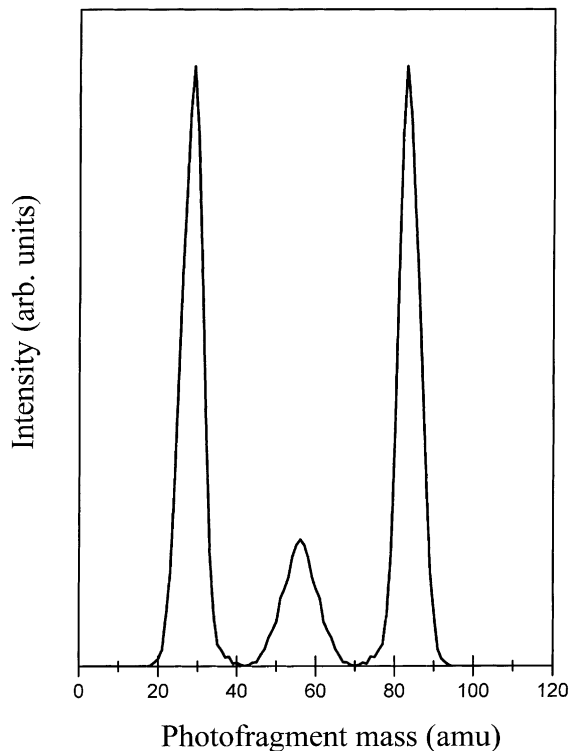


Fig. 4. Photofragment mass distribution resulting from excitation at 193 nm.

$43\,860\text{ cm}^{-1}$  were not recorded, dissociation was observed at wavelengths within that region.

Photofragment translational energy distributions were obtained at selected photon energies ranging from 5.17 to 6.42 eV. As shown in the representative photofragment mass distribution in Fig. 4, the  $\text{Si}_3 + \text{Si}$  mass channel was the major dissociation pathway, with a branching ratio of  $(\text{Si}_3 + \text{Si}) : (\text{Si}_2 + \text{Si}_2) = 6:1$ . The  $P(E_T)$  distributions for the  $\text{Si}_3 + \text{Si}$  mass channel are presented in Fig. 5; the signal for the  $\text{Si}_2 + \text{Si}_2$  mass channel was too low to gather  $P(E_T)$  distributions. All of the observed distributions are peaked towards low translational energy with a slight broadening of the distribution as the excitation energy is increased. In addition, the photofragment angular distributions were found to be isotropic.

Translational energy distributions that peak at low  $E_T$  and are weakly dependent upon the excitation energy are often a signature of a statistical, barrierless dissociation process. To test this more quantitatively, the experimental  $P(E_T)$  distributions were compared to those determined from phase space theory (PST), in which all product states permitted by conservation of energy and angular momentum are assumed to be equally probable. The calculation of photofragment translational energy distributions using this statistical theory has been described in detail elsewhere [30–32]. The PST distributions have been convoluted with a Monte Carlo simulation program to account for the apparatus parameters [7].

The results of applying PST to the dissociation of  $\text{Si}_4$  are shown as dashed lines in Fig. 5. The PST

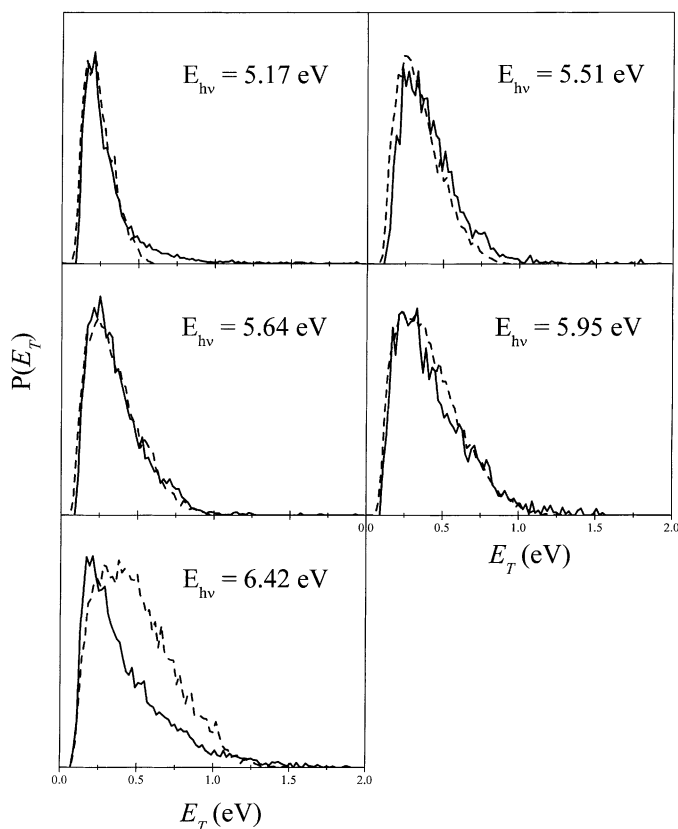


Fig. 5. Translational energy distributions for the  $\text{Si}_3 + \text{Si}$  channel at the excitation energies indicated as measured experimentally (solid) and modeled by phase space theory (dashed).

distributions were calculated using product rotational constants [33] and vibrational frequencies [11,16] for the  $\text{Si}_3(\tilde{X}^1\text{A}_1)$  state. As the  $P(E_T)$  distributions do not illustrate a clear onset to dissociation that would allow the direct determination of the dissociation energy,  $D_0$ , this value was varied to best reproduce the experimental distributions. We found that  $D_0 = 4.60$  eV resulted in good agreement with the distributions at 5.51, 5.64, and 5.95 eV, with error bars on  $D_0$  estimated at  $\pm 0.15$  eV. This dissociation energy is in agreement with more recent theoretical [21,22,34,35] and experimental [19] results. Employing the literature value of the heat of formation of Si [20] and the result for  $\text{Si}_3$  from the measurements by Schmude et al. [19] yields  $\Delta H_{f,0}^0(\text{Si}_4) = 6.75 \pm 0.24$  eV.

At 5.17 eV, the experimental  $P(E_T)$  distribution extends beyond  $E_T = 1.0$  eV, whereas the PST distribution cuts off at 0.6 eV, reflecting the maximum translational energy available for  $D_0 = 4.60$  eV. The experimental signal at higher  $E_T$  probably originates from multiphoton absorption; similar effects were seen in our study of carbon cluster photodissociation at photon energies just above the dissociation threshold [30]. On the other hand, at 6.42 eV (193 nm), the PST distribution predicts more translational energy than is seen in the experimental distribution, possibly reflecting production of electronically excited fragments in the experiment.

The generally good agreement between the PST and experimental  $P(E_T)$  distributions implies that the dissociation of  $\text{Si}_4$  is statistical and does not proceed over a sizeable exit barrier. Such a mechanism could occur if electronic excitation of  $\text{Si}_4$  were followed by internal conversion to the  $\text{Si}_4 \tilde{X}^1\text{A}_g$  ground state, where the lifetime is long enough so that energy randomization occurs prior to dissociation to  $\text{Si}_3 + \text{Si}$ . Statistical dissociation has been inferred in previous experimental and theoretical studies of  $\text{Si}_n^+$  cations from the observation of the lowest energy product channels and the general agreement between the products seen in photodissociation and in collision-induced dissociation [2,4,5,24,35]. Our results provide more detailed and direct evidence for statistical dissociation.

There are some issues of interest with regard to this mechanism. First, the lowest energy dissociation channel is  $\text{Si}_3(\tilde{X}^1\text{A}_1) + \text{Si}(^3\text{P})$ , a triplet channel that is spin-forbidden from the ground (singlet) state of  $\text{Si}_4$ . However, the  $\text{Si}_3(^3\text{A}'_2) + \text{Si}(^3\text{P})$  channel lies only 0.02 eV higher [14], and spin-allowed dissociation to this channel can occur. The energetic difference between these two dissociation channels is undetectable in our experiment, and differences in geometry and vibrational frequencies between the two electronic states of  $\text{Si}_3$  do not significantly alter the PST distributions. Hence, there is no way for us to definitively distinguish between these two channels.

Another point of interest is that  $\text{Si}_4$  has a planar rhombus structure, so that two Si–Si bonds need to be broken in order to form  $\text{Si}_3 + \text{Si}$  products. If both bonds were to break simultaneously, one would, in general, expect the reaction coordinate to pass through a three-center transition state and to have an exit barrier relative to the products, resulting in a  $P(E_T)$  distribution peaking noticeably away from  $E_T = 0$ . The observed distributions are inconsistent with this, suggesting either that concerted bond breaking occurs without an exit barrier, or that bond cleavage is sequential, so that product formation involves passage over a simple bond fission transition state. The application of electronic structure calculations to investigate the presence of a barrier for concerted bond dissociation would directly address this point.

There are several similarities between the photodissociation of  $\text{Si}_4$  and that of the carbon clusters  $\text{C}_4$ – $\text{C}_6$  [30]. Carbon clusters also undergo relatively facile multiphoton dissociation below the dissociation threshold, and above the threshold, the translational energy distributions could be fit by a combination of one-photon dissociation, described by PST, and multi-photon dissociation resulting in signal at high  $E_T$ . Carbon clusters also show nonzero, unstructured PFY signal over large wavelength ranges both above and below the dissociation threshold. Multiphoton effects were more pronounced in the carbon cluster work, with the multiphoton contribution to the  $P(E_T)$  distributions considerably stronger than for  $\text{Si}_4$ . However, the similarities between these systems outweigh the differences and are probably due to the same origin:

the large number of low-lying electronic states in carbon and silicon clusters that facilitate energy flow from an initially excited bright state.

#### 4. Conclusions

The photodissociation spectroscopy and dynamics of Si<sub>4</sub> have been studied by determining its photofragment yield spectrum, the masses of the photofragments, and the photofragment kinetic energy distribution. Si<sub>4</sub> undergoes photodissociation at photon energies well below the dissociation threshold, indicating that multiphoton dissociation is relatively facile, particularly when excitation is resonant with vibrational features of the <sup>1</sup>B<sub>1u</sub> ← <sup>1</sup>X̃<sup>1</sup>A<sub>g</sub> band of Si<sub>4</sub>. An unstructured PFY spectrum was found at photon energies above the dissociation threshold, with Si<sub>3</sub> + Si as the dominant dissociation channel. Photofragment kinetic energy distributions taken at several photon energies were found to peak near zero kinetic energy, and could be reasonably well-modeled (except at 193 nm) using phase space theory. From this we conclude that Si<sub>4</sub> dissociation is statistical and barrierless, most likely involving internal conversion from the initially excited state to the ground state followed by fragmentation. From the parameters used in fitting the model PST distributions to the experimental distributions, the dissociation energy of Si<sub>4</sub> was determined to be 4.60 ± 0.15 eV, and ΔH<sub>f,0</sub><sup>0</sup>(Si<sub>4</sub>) = 6.75 ± 0.24 eV.

#### Acknowledgements

This research is supported by the National Science Foundation under Grant No. DMR-9814677.

#### References

- [1] M.L. Mandich, in: G.W.F. Drake (Ed.), *Atomic, Molecular, and Optical Physics Handbook*, AIP Press, Woodbury, 1996, p. 452.
- [2] L.A. Bloomfield, R.R. Freeman, W.L. Brown, *Phys. Rev. Lett.* 54 (1985) 2246.
- [3] Y. Liu, Q.-L. Zhabg, F.K. Tittel, R.F. Curl, R.E. Smalley, *J. Chem. Phys.* 85 (1986) 7434.
- [4] Q.-L. Zhang, Y. Liu, R.F. Curl, F.K. Tittel, R.E. Smalley, *J. Chem. Phys.* 88 (1988) 1670.
- [5] M.F. Jarrold, J.E. Bower, *J. Phys. Chem.* 92 (1988) 5702.
- [6] K.D. Rinnen, M.L. Mandich, *Phys. Rev. Lett.* 69 (1992) 1823.
- [7] R.E. Continetti, D.R. Cyr, D.L. Osborn, D.J. Leahy, D.M. Neumark, *J. Chem. Phys.* 99 (1993) 2616.
- [8] W. Weltner Jr., D. McLeod Jr., *J. Chem. Phys.* 41 (1964) 235.
- [9] J. Fulara, P. Freivogel, M. Grutter, J.P. Maier, *J. Phys. Chem.* 100 (1996) 18042.
- [10] E.C. Honea, A. Ogura, C.A. Murray, K. Raghavachari, W.O. Sprenger, M.F. Jarrold, W.L. Brown, *Nature* 366 (1993) 42.
- [11] S. Li, R.J. Vanzee, W. Weltner, K. Raghavachari, *Chem. Phys. Lett.* 243 (1995) 275.
- [12] C.B. Winstead, K.X. He, D. Grantier, T. Hammond, J.L. Gole, *Chem. Phys. Lett.* 181 (1991) 222.
- [13] O. Cheshnovsky, S.H. Yang, C.L. Pettiette, M.J. Craycraft, Y. Liu, R.E. Smalley, *Chem. Phys. Lett.* 138 (1987) 119.
- [14] C.S. Xu, T.R. Taylor, G.R. Burton, D.M. Neumark, *J. Chem. Phys.* 108 (1998) 1395.
- [15] C.C. Arnold, D.M. Neumark, *J. Chem. Phys.* 99 (1993) 3353.
- [16] C.M. Rohlfing, K. Raghavachari, *J. Chem. Phys.* 96 (1992) 2114.
- [17] A. Rubio, J.A. Alonso, X. Blase, L.C. Balbas, S.G. Louie, *Phys. Rev. Lett.* 77 (1996) 247.
- [18] K. Jackson, M.R. Pederson, D. Porezag, Z. Hajnal, T. Frauenheim, *Phys. Rev. B* 55 (1997) 2549.
- [19] R.W. Schmude, Q. Ran, K.A. Gingerich, J.E. Kingcade, *J. Chem. Phys.* 102 (1995) 2574.
- [20] M.W. Chase and National Institute of Standards and Technology (US), *NIST-JANAF thermochemical tables*, fourth ed. American Chemical Society; American Institute of Physics for the National Institute of Standards and Technology, Washington, DC, Woodbury, NY, 1998.
- [21] R. Fournier, S.B. Sinnott, A.E. Depristo, *J. Chem. Phys.* 97 (1992) 4149.
- [22] L.A. Curtiss, P.W. Deutsch, K. Raghavachari, *J. Chem. Phys.* 96 (1992) 6868.
- [23] K. Raghavachari, *J. Chem. Phys.* 84 (1986) 5672.
- [24] K. Raghavachari, C.M. Rohlfing, *Chem. Phys. Lett.* 143 (1988) 428.
- [25] R.D. Kay, L.M. Raff, D.L. Thompson, *J. Chem. Phys.* 93 (1990) 6607.
- [26] D.J. Leahy, D.L. Osborn, D.R. Cyr, D.M. Neumark, *J. Chem. Phys.* 103 (1995) 2495.
- [27] D.L. Osborn, H. Choi, D.H. Mordaunt, R.T. Bise, D.M. Neumark, C.M. Rohlfing, *J. Chem. Phys.* 106 (1997) 3049.
- [28] D.L. Osborn, D.J. Leahy, D.R. Cyr, D.M. Neumark, *J. Chem. Phys.* 104 (1996) 5026.
- [29] D.P. de Bruijn, J. Los, *Rev. Sci. Instrum.* 53 (1982) 1020.

- [30] H. Choi, R.T. Bise, A.A. Hoops, D.H. Mordaunt, D.M. Neumark, *J. Phys. Chem. A* 104 (2000) 2025.
- [31] P. Pechukas, J.C. Light, *J. Chem. Phys.* 42 (1965) 3281.
- [32] P.J. Robinson, K.A. Holbrook, *Unimolecular Reactions*, Wiley/Interscience, New York, 1972.
- [33] D.W. Dean, J.R. Chelikowsky, *Theor. Chem. Acc.* 99 (1998) 18.
- [34] J.C. Grossman, L. Mitas, *Phys. Rev. Lett.* 74 (1995) 1323.
- [35] A.A. Shvartsburg, M.F. Jarrold, B. Liu, Z.Y. Lu, C.Z. Wang, K.M. Ho, *Phys. Rev. Lett.* 81 (1998) 4616.